

<https://doi.org/10.1038/s41525-025-00523-2>

Biallelic variants in *BBOX1* cause L-Carnitine deficiency and elevated γ -butyrobetaine



Xiao Li^{1,2,3,11}, Mehdi Yeganeh^{4,11}, Graham Sinclair⁵, Jill Mwenifumbo⁶, Karen J. Jacob⁶, Laura Arbour⁷, Anna Lehman^{6,8}, Bojana Rakic⁵, Frédéric M. Vaz^{9,10}, Gabriella Horvath^{4,8}, Maja Tarailo-Graovac^{1,2,3} ✉ & Sylvia Stockler-Ipsiroglu⁴ ✉

Gamma-butyrobetaine hydroxylase (BBOX1) catalyses the last step of carnitine biosynthesis, converting γ -butyrobetaine (γ -BB) into L-carnitine. Here we show, for the first time, that biallelic variants in *BBOX1* are associated with decreased levels of L-carnitine and increased plasma levels of γ -BB in three patients from two unrelated families presenting with myopathic, neurodevelopmental, and late-onset psychiatric manifestations. Using a knockout *C. elegans* model of *BBOX1* homolog, *gbh-1*, and strains harboring patient-derived variants (*gbh-1*(D72G) for p.Asp59Gly, *gbh-1*(G283R) for p.Gly263Arg, and *gbh-1*(G247Vfs6) for p.Gly227Valfs*6), we show very low L-carnitine levels and significantly elevated γ -BB in c.675delA and c.787G>A mutants, and moderately elevated γ -BB in c.176A>G. Furthermore, we observed a lethal embryonic phenotype for the *gbh-1* loss-of-function strains, which was rescued upon L-carnitine supplementation. Our study provides novel insights into the clinical and biochemical consequences of BBOX1-related L-carnitine biosynthesis deficiency and establishes *C. elegans* as a model to study the effects of BBOX1 deficiency.

L-carnitine is essential for transporting long-chain fatty acids into the mitochondria for β -oxidation, which is essential for cardiac and skeletal muscle energy metabolism and hepatic ketogenesis during fasting periods. L-carnitine also plays a role in shuttling partially degraded fatty acids from the peroxisome for further degradation, and in acting as a buffer to maintain adequate levels of free CoA¹.

L-carnitine homeostasis is maintained through endogenous synthesis and dietary intake with enteral absorption and renal reabsorption via sodium-dependent organic cation/carnitine transporter-2 (*SLC22A5*)². Endogenous synthesis of L-carnitine occurs mainly in the liver, brain, and kidneys in a four-step enzymatic pathway, with 6-N-trimethyllysine (TML) as the initial substrate. γ -butyrobetaine hydroxylase (BBOX1), a cytosolic dimeric protein, catalyzes the last step converting γ -butyrobetaine (γ -BB) to L-carnitine^{3,4} (Fig. 1A).

Although inborn errors of L-carnitine transport and utilization have been well described in the literature⁵, reports on defective endogenous L-carnitine biosynthesis are limited. Celestino-Soper et al. identified a deletion in exon 2 of the X-linked trimethyl lysine hydroxylase gene (*TMLHE*), which encodes the enzyme catalyzing the first step in L-carnitine synthesis, in an individual with autism⁶. They later reported an increased prevalence of this deletion in male-male multiplex autism families, suggesting a potential link between TMLHE deficiency and autism risk⁷. Rashidi-Nezhad et al. described a 42-month-old female with microcephaly, developmental delay, and moderately low carnitine levels who had a homozygous 221 Kb deletion in 11p14.2, which includes *BBOX1*, but investigations to validate the biochemical phenotype were not performed⁸.

Here, we report three *BBOX1* variants in three patients from two unrelated families with variable muscular developmental and psychiatric

¹Department of Biochemistry and Molecular Biology, Cumming School of Medicine, University of Calgary, Calgary, AB, Canada. ²Department of Medical Genetics, Cumming School of Medicine, University of Calgary, Calgary, AB, Canada. ³Alberta Children's Hospital Research Institute, University of Calgary, Calgary, AB, Canada. ⁴Department of Pediatrics, University of British Columbia, Division of Biochemical Genetics, BC Children's Hospital, Vancouver, BC, Canada. ⁵Department of Pathology and Laboratory Medicine, University of British Columbia, Biochemical Genetics Laboratory Children's & Women's Hospital, Vancouver, BC, Canada. ⁶Department of Medical Genetics, University of British Columbia, Vancouver, BC, Canada. ⁷Department of Medical Genetics, and the Island Medical Program, University of British Columbia, Victoria, BC, Canada. ⁸Adult Metabolic Diseases Clinic, Department of Medicine, Vancouver General Hospital, Vancouver, BC, Canada. ⁹Amsterdam UMC location University of Amsterdam, Department of Laboratory Medicine and Pediatrics, Laboratory Genetic Metabolic Diseases, Emma Children's Hospital, Amsterdam, The Netherlands. ¹⁰Amsterdam Gastroenterology Endocrinology Metabolism, Inborn Errors of Metabolism, Amsterdam, The Netherlands. ¹¹These authors contributed equally: Xiao Li, Mehdi Yeganeh. ✉ e-mail: maja.tarailograovac@ucalgary.ca; sstockler@cw.bc.ca

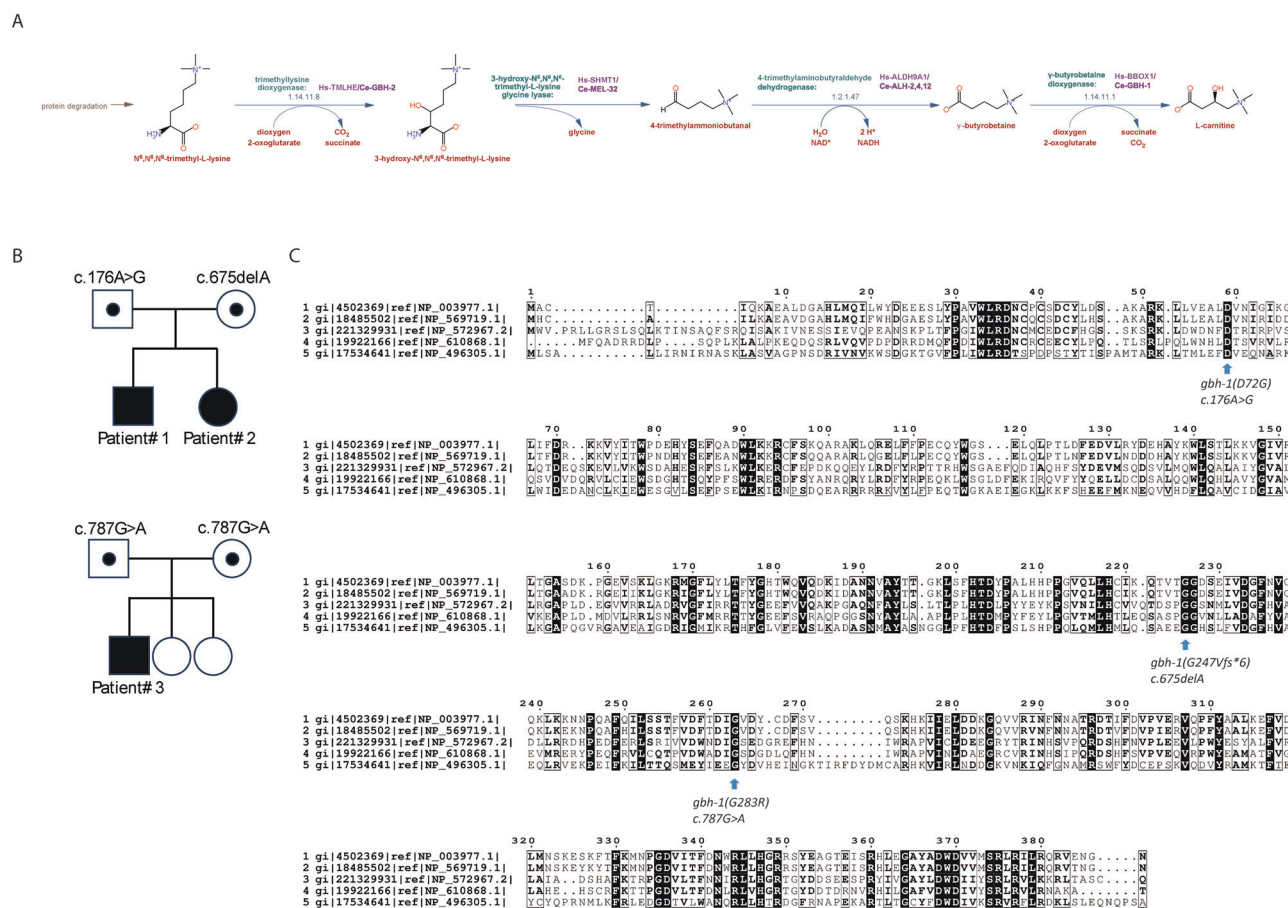


Fig. 1 | Biochemical pathway and cross-species conservation of BBOX1/GBH-1.

A L-Carnitine Biosynthesis Pathway: Four steps of the L-carnitine biosynthesis pathway, catalyzed by respective conserved orthologous enzymes in humans (Hs) and *C. elegans* (Ce), ended by the production of L-carnitine by BBOX1/GBH-1; Pathway was generated and adapted from MetaCyc database²⁸ (<https://metacyc.org/pathway?orgid=META&id=PWY-6100&ENZORG=TAX-9606&detail-level=3>).

B Patient pedigrees; **C** BBOX1/GBH-1 sequence conservation and variant modeling.

presentations, reduced plasma L-carnitine levels, as well as elevated γ -BB levels. To accurately study the pathogenicity of these variants, we employed *Caenorhabditis (C.) elegans* as a model organism to determine the specific phenotype related to patients' *BBOX1* variants. Our results for the first time demonstrate that biallelic variants in *BBOX1* cause a clinical and biochemical phenotype that is consistent with a deficiency in endogenous carnitine synthesis.

Results

Case reports

Patients 1 and 2 are a 30-year-old man and his 26-year-old sister, the only two children of healthy non-consanguineous parents of European ancestry with an unremarkable family history (Fig. 1B).

Patient 1 presented first during his infancy with episodes of irritability and lethargy associated with prolonged fasting that were responsive to feeding. Hypoglycemia was not documented, and symptoms improved as he reached childhood. At 6 years, he developed fine motor coordination delay, swallowing difficulty with frequent choking, bilateral ptosis, as well as exercise intolerance, intermittent muscle soreness, and generalized muscle weakness affecting mainly his trunk and proximal muscles. Narcolepsy-like attacks could happen at any time during the day. He also developed a mild cardiomyopathy that resolved by the age of 18 years. Since the age of 23 years, he has been seen for episodes of psychosis and one episode of ketamine-induced seizures.

The sequence alignment suggests the conservation of the BBOX1 across various species, including humans, mice, zebrafish, fruit flies, and *C. elegans* (GBH-1) (from top to bottom). The positions of amino acid residues altered in patient-derived variants are invariant. CRISPR/Cas9-assisted gene editing in *C. elegans* models the human variants p.Asp59Gly, p.Gly263Arg, and p.Gly227Valfs*6, corresponding to D59G, G283R, and G247Vfs*6 in GBH-1, to examine their impact on the function of the L-carnitine biosynthesis pathway.

Electromyogram and nerve conduction (EMG-NCV) studies, echocardiogram, and electrocardiogram were unremarkable. Brain magnetic resonance imaging (MRI) performed at age 9 years showed nonspecific T2 signal abnormalities in the white matter. Plasma CK levels were normal. Biochemical genetic workup revealed persistently low levels of serum free carnitine. L-carnitine transporter and fatty acid oxidation-related L-carnitine deficiency were ruled out by normal renal excretion fraction of L-carnitine (Table 1) and by demonstration of a normal acylcarnitine profile in cultured fibroblasts incubated with palmitic acid and L-carnitine (Table S1). Histopathology examination of a quadriceps biopsy showed type 1 muscular fiber predominance with normal immunostaining and Gomori trichrome staining. Mitochondrial morphology and respiratory chain enzyme activity were normal, and there was no evidence for a possible storage disease or an inflammatory myopathy. Muscle carnitine content was normal, but the patient was on L-carnitine supplementation at the time of biopsy (data not shown). Molecular testing for facioscapulohumeral muscular dystrophy was negative.

A gene panel (Labcorps MNG), including the mitochondrial genome and 431 nuclear genes associated with defects in cellular energy energetics, revealed two compound heterozygous variants in *BBOX1*: NM_003986.3:c.176A>G (p.Asp59Gly) paternally inherited, and NM_003986.3:c.675delA (p.Gly227Valfs*6) maternally inherited (Table 1 and Fig. 1B). Additional heterozygous variants included a variant of uncertain significance in *RYR1* NM_000540.3:c.10171G>A (p.Glu3391Lys)

Table 1 | Biochemical and clinical findings in 3 patients with *BBOX1* variants

	Patient #1	Patient #2	Patient #3
<i>BBOX1</i> Variants			
paternal	NM_003986.3:c.176A>G (p.Asp59Gly)	NM_003986.3:c.176A>G (p.Asp59Gly)	NM_003986.3:c.787G>A (p.Gly263Arg)
maternal	NM_003986.3:c.675delA (p.Gly227Valfs*6)	NM_003986.3:c.675delA (p.Gly227Valfs*6)	NM_003986.3:c.787G>A (p.Gly263Arg)
Biochemical results			
(s) Total carnitine (30–69 µmol/L)			
Prior to L-carnitine supplementation	15.7	11.3 (dbs)	12.0
During L-carnitine supplementation	17.3	8.1 (s) 28	59
(s) Free carnitine (16–60 µmol/L)			
Prior to L-carnitine supplementation	12	4.1 (dbs) 5.7 (s)	8.0
During L-carnitine supplementation	14.8	18.2	49.8
(u) Fractional carnitine excretion (<5%)			
Prior to L-carnitine supplementation	1.0	1.0	0.7, 2.9
During L-carnitine supplementation	(nd)	(nd)	(nd)
(p) 6-N-TML (0.2–1.2 µmol/L)			
Prior to L-carnitine supplementation	(nd)	0.39	0.50
During L-carnitine supplementation	0.52	(nd)	0.60
(p) γ-BB (0.3–1.4 µmol/L)			
Prior to L-carnitine supplementation	(nd)	5.50	13.20
During L-carnitine supplementation	9.40	(nd)	10.90
HTML/TML* (0.1–1.4)			
Prior to L-carnitine supplementation	(nd)	0.08	0.14
During L-carnitine supplementation	0.17	(nd)	0.19
Clinical findings			
Hypoglycemia	+	-	-
Fasting intolerance	+	-	-
Fine motor delay	+	+	+
Speech delay	-	-	+
Autism	-	-	+
Swallowing difficulty	++	-	-
Muscle weakness	+	+	+
Fatigability	+	+	+
Muscle wasting	+	-	-
Ptosis	+	-	-
Learning difficulty	-	-	+
Psychosis	+	-	-
Anxiety	-	+	+

dbs dry blood spot, nd not determined, p plasma, s serum, u urine,

γ-BB gamma-butyrobetaine, 6-N-TML (6-N-trimethyllysine), HTML/TML hydroxytrimethyllysine/trimethyllysine ratio.

*HTML/TML ratio is characteristically reduced in TMLHE-related carnitine biosynthesis defect.

and *ACADL* NM_001608.4:c.1018_1019del (p.His340Tyrfs*16). Mitochondrial genome sequencing detected a homoplasmic variant of uncertain significance in *MT-RNR2* (m.2672A>G) in him and his asymptomatic mother.

Measurement of carnitine biosynthesis intermediates was done while the patient was on L-carnitine supplementation (100 mg/kg), showing elevation of γ -BB in plasma (Table 1) and urine (data not shown) while plasma L-carnitine levels were within the normal range.

Patient 2 was seen during her childhood for migraine headaches, coordination difficulty, and dyslexia, requiring assistance at school. At 4 years of age, she started having muscle weakness, exercise intolerance, and impaired gait. As a young adult, she developed severe anxiety. Brain and spine MRI, EMG-NCS, echocardiogram, and electrocardiogram were unremarkable. She had low serum L-carnitine levels in the presence of a normal renal extraction fraction of carnitine (Table 1). Family variant testing, using Sanger sequencing, detected the same *BBOX1* variants as in her brother, who also was found to have elevated plasma γ -BB levels (Table 1).

Patient 3 is a 15-year-old boy born to a healthy First Nations couple following a normal pregnancy. He has two younger, healthy, and normally developing sisters (Fig. 1B). First Nations are one of three distinct Indigenous populations of Canada. The patient presented at age 4 years with language delay, learning difficulties and was later diagnosed with autism spectrum disorder. There was a history of fatigability and intolerance to physical exercise. Echocardiogram and electrocardiogram, as well as a chromosomal microarray and fragile X syndrome molecular testing, were normal. Biochemical genetic workup showed persistently low free carnitine levels both on dried bloodspots and in serum, in the presence of normal renal L-carnitine fractional excretion (Table 1).

Genome sequencing (Silent Genomes Project <https://www.bcchr.ca/silent-genomes-project>) revealed a homozygous variant of uncertain significance in *BBOX1* NM_003986.3:c.787G>A (p.Gly263Arg) (Fig. 1B). In addition, a homozygous variant in *CPT1A* NM_001876.4:c.1436C>T (p.Pro479Leu) was identified. This variant is very rare in gnomADv4.1.0 (0.00003036) and in a TopMED Freeze 10 database (0.000046389); however, it is quite common in an Indigenous Background Variant Library (IBVL; <https://www.bcchr.ca/silent-genomes-project/ibvl>), where variant allele frequency (VAF) is close to 11% (0.107388). 5% of the Arctic Indigenous and coastal First Nations populations of British Columbia are homozygous for this variant. It is associated with a mild form of carnitine palmitoyl transferase I deficiency, putting homozygous individuals at risk for fasting hypoglycemia^{9,10}. The symptoms observed in patient 3 have not been associated with this variant.

Measurement of L-carnitine biosynthesis intermediates revealed elevated γ -BB levels in plasma and urine (Table 1). Oral supplementation of L-carnitine (50–100 mg/kg/day) normalized serum free L-carnitine levels and improved fatigability and muscle weakness. This patient was lost to follow-up, and we are unaware of his most recent clinical status.

BBOX1 variants

The two missense variants NM_003986.3:c.176A>G (p.Asp59Gly) (family 1) and NM_003986.3:c.787G>A (p.Gly263Arg) (family 2) were predicted to be damaging by three in silico metrics (SIFT; Sorting Intolerant From Tolerant¹¹, PolyPhen-2¹², and CADD; Combined Annotation Dependent Depletion)¹³ (Table S2). The frameshift variant NM_003986.3:c.675delA

(p.Gly227Valfs*6) (family 1) leads to a premature stop codon and is predicted to code for a truncated protein of 231 amino acids (40% of the C-terminus sequence removed). All three variants are absent or ultrarare in genomic databases, like gnomADv4.1.0 and TOPMed Freeze 10 (Table S2). We have also checked all three variants in the current version of IBVL (Release 1.1) (<https://www.bcchr.ca/silent-genomes-project/ibvl>), and while p.(Asp59Gly) and p.(Gly227ValfsTer6) are completely absent, the p.(Gly263Arg) variant was present at a population frequency of 0.010309300 (12 heterozygous and no homozygous individuals) in the IBVL (<https://www.bcchr.ca/silent-genomes-project/ibvl>), suggesting that it may be a founder variant of community significance.

Investigation of orthologous *gbh-1* variants in *C. elegans*

Leveraging the conservation of metabolic pathways between humans and *C. elegans*¹⁴ (Fig. 1A), we sought to investigate the functional implications of the identified *BBOX1* variants in a *C. elegans* model. The orthologous enzyme in *C. elegans*, GBH-1, shares 33% sequence identity with human BBOX1 (Fig. 1C). This conservation extends to the specific amino acid residues affected by the identified variants in our patients (Fig. 1B, C).

Employing CRISPR/Cas9, we first generated a complete *gbh-1* knockout model, *gbh-1(ko)*, and then introduced variants equivalent to those identified in our patients: *gbh-1(D72G)* for p.Asp59Gly, *gbh-1(G283R)* for p.Gly263Arg, and *gbh-1(G247Vfs6)* for p.Gly227Valfs*6 (Table 2 and Fig. S1).

Phenotype of *gbh-1(ko)* in *C. elegans*

We tested the impact of these variants on *C. elegans* growth and reproductive fitness under various nutritional conditions. To this end, different strains of *E. coli* as a nutritional source were used as a food source, and starvation–refeeding experiments were performed with and without additional L-carnitine supplementation. Standard conditions involved *E. coli* OP50 (a uracil auxotroph providing controlled bacterial growth), whereas *E. coli* BW25113 (Δ *caiA*)—which is not a uracil auxotroph and thus forms thick bacterial lawns—was used to create an L-carnitine-depleted environment¹⁵.

gbh-1(ko) worms cultured under standard conditions (“thin OP50” plates) exhibited no growth abnormalities. However, embryonic viability was notably reduced with hatch rates varying from 0 to 46% (Fig. 2A). Because L-carnitine is required for mitochondrial β -oxidation of fatty acids—especially during fasting when fatty acid catabolism is prioritized¹⁶—we tested whether nutrient deprivation would exacerbate this phenotype. Indeed, after 2–3 days of starvation, refeeding *gbh-1(ko)* mutants on thin OP50 plates yielded consistently reduced embryonic viability, whereas wild-type N2 worms maintained near 100% hatch rates (Fig. 2B, Fig. S2A, B). Increasing bacterial density on OP50 plates (“thick OP50”) or switching to rich bacterial strains such as HB101 or BW25113 restored *gbh-1(ko)* hatch rates to wild-type levels (Fig. 2B, C). However, refeeding starved *gbh-1(ko)* on thick BW25113 (Δ *caiA*) plates failed to rescue embryonic lethality (Fig. 2D). Supplementing these plates with exogenous L-carnitine, by contrast, completely rescued hatch rates (Fig. 2B–D).

L-carnitine deficiency as the specific cause of pathogenicity associated with *gbh-1* variants

We performed the same set of experiments in *C. elegans* strains carrying the variants equivalent to those identified in our patients: *gbh-1(D72G)* for p.Asp59Gly, *gbh-1(G283R)* for p.Gly263Arg, and *gbh-1(G247Vfs6)* for p.Gly227Valfs*6.

Table 2 | Genetic variants in humans and engineered *C. elegans* strains using CRISPR/Cas9

Human NM_003986.3	Protein Sequence Change	<i>C. elegans</i> Ortholog	Sequence Changes in <i>gbh-1</i>
c.787G>A	Gly263Arg	<i>gbh-1(G283R)</i>	GGA->CGT
c.176A>G	Asp59Gly	<i>gbh-1(D72G)</i>	GAC>GGA
c.675delA	Gly227Valfs*6+VIQKL*	<i>gbh-1(G247Vfs*6)+VIQKL*</i>	deletion of GACATAGTCTATTTGTT and insertion of GTGATTCAGAAATTGTAG encoding VIQKL*
Knockout	No protein	<i>gbh-1(ko)</i>	Deletion of CDS

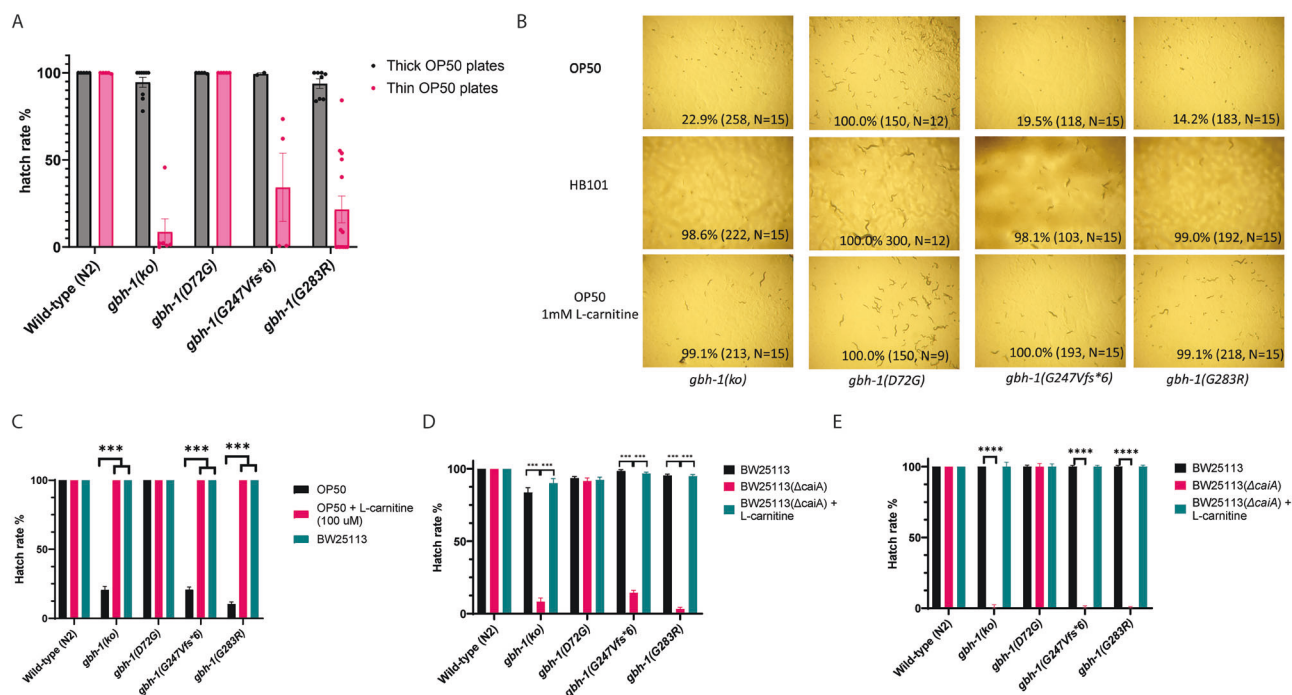


Fig. 2 | L-carnitine rescues nutritional deficits in *C. elegans gbh-1* mutants.

A Hatch rate analysis on thin versus thick *E. coli* OP50 lawns shows semi-lethality in *gbh-1(ko)*, *G247Vfs*6*, and *G283R* mutants, but not *D72G*, under standard conditions. Enhanced survival on thick OP50 lawns suggests semi-lethality is mitigated by improved nutritional availability; **B** Starvation-refeeding experiments conducted on thin OP50 plates reveal consistent F1 embryonic lethality in *gbh-1(ko)*, *G247Vfs*6*, and *G283R* strains. When refeeding occurs with the HB101 *E. coli* strain, known for dense lawn formation, lethality is rescued. Supplementing OP50 with 1mM L-carnitine also rescues lethality of these strains on OP50; **C** In a similar starvation-refeeding experiments to (**B**), F1 embryonic lethality of *gbh-1(ko)*,

*G247Vfs*6*, and *G283R* strains is rescued by supplementation with 100 μ M L-carnitine, or the use of the BW25113 bacterial strain, which also forms a dense lawn; **D** Starvation-refeeding experiments conducted on a BW25113(Δ caia) plates resulted in the F1 embryonic lethality phenotype for *gbh-1(ko)*, *G247Vfs*6*, and *G283R* strains; **E** Without prior starvation, *gbh-1(ko)*, *G247Vfs*6*, and *G283R* worms demonstrate consistent F1 embryonic lethality on BW25113(Δ caia) plates. The lethality is consistent across *gbh-1* mutants except for *D72G*. **A** and **C–E** Statistical significance: *** $p < 0.001$ and **** $p < 0.0001$ (unpaired *t*-test). Bar graphs represent hatch rates under various conditions. Error bars represent the standard error of the mean.

Under standard conditions on thin OP50 plates, *gbh-1(G283R)* and *gbh-1(G247Vfs*6)* genocopied the knockout, exhibiting nutrition-dependent embryonic lethality (Fig. 2A). They also experienced heightened lethality after starvation and refeeding on OP50, but nutrient-rich conditions or exogenous L-carnitine supplementation rescued the phenotype (Fig. 2B, C). These results strongly suggest that *gbh-1(G283R)* and *gbh-1(G247Vfs*6)* are functional alleles. By contrast, *gbh-1(D72G)* mutants displayed wild-type embryonic viability under all conditions tested (Fig. 2A–C). Similarly, double-heterozygous-mutant worms carrying both the *D72G* and *G247Vfs*6* alleles (modeling the two patients carrying the compound heterozygous variants) showed no embryonic lethality, even under prior starvation (Fig. S2C).

To confirm that L-carnitine deficiency specifically underlies the phenotype of these variants, we tested these strains on BW25113 (Δ caia). Wild-type BW25113 fully supports these mutants, achieving 100% hatch rates (Fig. 2C, D). However, *gbh-1(G283R)* and *gbh-1(G247Vfs*6)* worms grown on BW25113 (Δ caia) plates had extremely low hatch rates (0–10%), which were restored to 100% upon L-carnitine supplementation, exhibiting the same susceptibility and rescue pattern as the *gbh-1(ko)* worms (Fig. 2C, D, Fig. S2D). As in other experiments, *gbh-1(D72G)* behaved like the wild type.

Notably, even without prior starvation, culturing *gbh-1(ko)* on BW25113 (Δ caia) resulted in complete embryonic lethality (0% hatch) (Fig. 2E, Fig. S2E), suggesting that L-carnitine is specifically required for embryonic viability in worms lacking *gbh-1*.

γ -butyrobetaine (γ -BB) toxicity in *gbh-1* variants

To explore whether excess γ -BB selectively causes negative fitness effects, *gbh-1(ko)*, *gbh-1(G247Vfs*6)*, *gbh-1(G283R)*, and *gbh-1(D72G)* strains were

cultured in the presence of γ -BB, using the BW25113 *E. coli* strain as a nutritional source, a nutritional environment under which these mutants typically exhibit a 100% hatch rate. Exposure to 1 mM γ -BB resulted in total embryonic lethality in the *gbh-1(ko)*, *gbh-1(G247Vfs*6)*, and *gbh-1(G283R)* mutants (Fig. 3A), while the *gbh-1(D72G)* mutant strain demonstrated no lethality at concentrations up to 50 mM (Fig. 3B).

Further, growth assays conducted in liquid culture revealed no significant growth delays for the *gbh-1(D72G)* mutants compared to the wild-type N2 strain, even at elevated γ -BB concentrations (Fig. S3).

Metabolic profile of *gbh-1* mutants

To further characterize the metabolic profile in our *C. elegans* model, we used high-performance liquid chromatography-mass spectrometry (HPLC-MS) analyses. The *gbh-1(ko)*, *gbh-1(G247Vfs*6)*, and *gbh-1(G283R)* strains exhibited profound accumulation of γ -BB, with levels more than 50-fold above those seen in wild-type N2 nematodes (Fig. 4A). The *gbh-1(D72G)* mutants showed a comparably modest but consistent and statistically significant increase in γ -BB (Fig. 4A, Fig. S4A). We also observed complete L-carnitine deficiency as a sign of complete impairment of L-carnitine synthesis in *gbh-1(ko)*, *gbh-1(G247Vfs*6)*, and *gbh-1(G283R)* mutants (Fig. 4B and Fig. S4A), while we did not observe a difference in L-carnitine level in the *gbh-1(D72G)* worms.

Further metabolic profiling enabled the identification of precursors to γ -BB and a diverse range of acylcarnitine species, from C2 to C20 (Fig. S5B–F). The notable depletion of acylcarnitines in *gbh-1(ko)*, *gbh-1(G247Vfs*6)*, and *gbh-1(G283R)* mutants—contrasted with the relatively unchanged levels of upstream precursors of the L-carnitine synthesis pathway—highlights the specific blockade encountered in the biosynthetic process (Fig. 4C).

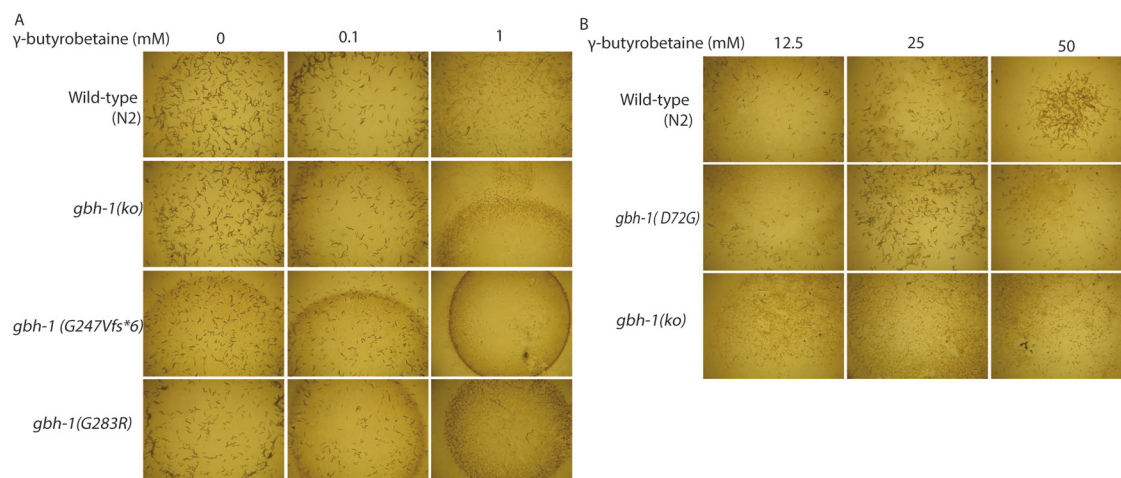


Fig. 3 | Sensitivity of *gbh-1* mutant *C. elegans* strains to γ -butyrobetaine exposure. **A** Wild-type N2, *gbh-1(ko)*, *gbh-1(G247Vfs*6)*, and *gbh-1(G283R)* worms subjected to different concentrations of γ -butyrobetaine. A complete F1 embryonic lethality for *gbh-1(ko)*, *gbh-1(G247Vfs*6)*, and *gbh-1(G283R)* worms at a 1 mM

concentration of γ -butyrobetaine; **B** *gbh-1(D72G)* worms show robustness against γ -butyrobetaine, with survival unaffected even at elevated concentrations up to 50 mM, similar to N2 worms.

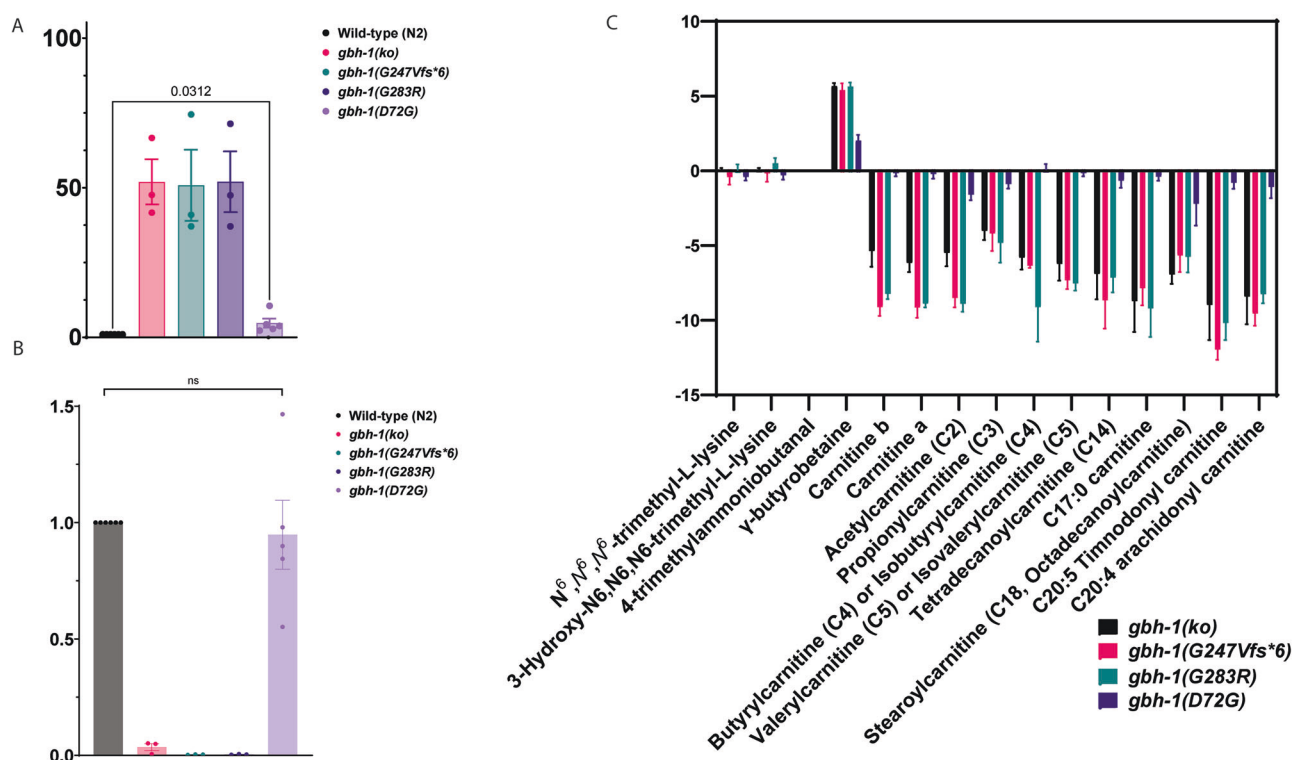


Fig. 4 | Metabolic alterations in *gbh-1* mutant strains revealed by HPLC-MS. **A** A substantial accumulation of γ -butyrobetaine in *gbh-1(ko)*, *gbh-1(G247Vfs*6)*, and *gbh-1(G283R)* mutants, exhibiting over a 50-fold increase compared to wild-type N2 worms. A modest increase of approximately 2-fold and statistically significant (non-paired *t*-test) is observed in *gbh-1(D72G)* mutants. The y-axis represents fold changes; **B** L-carnitine is undetectable in *gbh-1(ko)*, *gbh-1(G247Vfs*6)*, and *gbh-1(G283R)* strains, indicating a disruption in its biosynthesis. In contrast, *gbh-1(D72G)* worms maintain comparable L-carnitine levels to N2 worms. The y-axis

represents fold changes; **C** The acylcarnitine spectrum is markedly absent in *gbh-1(ko)*, *gbh-1(G247Vfs*6)*, and *gbh-1(G283R)* worms, as reflected by non-detectable levels across these mutants. Metabolites upstream of γ -butyrobetaine do not display significant changes. The y-axis represents the log2 fold change. **A** & **B** Statistical significance: $p = 0.0312$ and $p > 0.05$ (ns) (unpaired *t*-test). Bar graphs represent the normalized ratio against metabolite quantification of wild-type samples in each dataset. Error bars represent the standard error of the mean.

Discussion

We report 3 probands from two unrelated families with rare *BBOX1* variants, L-carnitine deficiency, and elevated levels of plasma γ -BB, indicative of a causative effect of the *BBOX1* variants affecting the final stage of the L-carnitine biosynthetic pathway.

Myopathic, neurodevelopmental, and late-onset psychiatric manifestations are clinical hallmarks in our patients. While myopathic manifestations are also found in other types of L-carnitine deficiency, e.g., *SLC22A5*-related carnitine transporter deficiency, additional neurodevelopmental and psychiatric manifestations seem to be specifically related to *BBOX1*

deficiency. Immune-mediated downregulation of BBOX1 in a mouse model with schizophrenia and the association of BBOX1 polymorphisms with increased schizophrenia susceptibility in the Korean population¹⁷ support a causal association of BBOX1 deficiency with autism spectrum and psychiatric disorders.

Treatment with L-carnitine resulted in the correction of L-carnitine deficiency in all our patients. In patient 3, the normalization of plasma L-carnitine levels was accompanied by improvement of muscle weakness and fatigability, while the degree of γ -BB accumulation in the plasma remained unchanged upon L-carnitine supplementation. This finding suggests that there is no end product-controlled L-carnitine synthesis in BBOX1 deficiency, which is in line with previous experimental data in rats and humans⁴.

BBOX1 is a protein-coding gene that contains nine exons and is located on the short arm of chromosome 14. The human cDNA contains an open reading frame encoding a polypeptide of 387 amino acids¹⁸. BBOX1 variants predicted to code for truncated proteins, such as NM_003986.3:c.688G>A (p.Glu230*) and NM_003986.3:c.330dup (p.Pro111Serfs*18), have been found in homozygous individuals in the population database gnomAD, posing the question of whether these individuals may have milder phenotypes, possibly due to modifier effects. The clinical and biochemical features of the 3 patients reported here demonstrate that at least certain BBOX1 variants cause a significant phenotype affecting neuromuscular and psychomotor development and functioning.

To further investigate the pathogenicity of the BBOX1 variants identified in our patients, we engineered a *C. elegans* knockout model devoid of the entire coding sequence of the BBOX1 ortholog *gbh-1* (*ko*), and strains bearing patient-derived BBOX1 variants, including *gbh-1*(G283R), *gbh-1*(G247Vfs*6), and *gbh-1*(D72G), which are orthologous to the human BBOX1 variants p.Gly263Arg, p.Gly227Valfs*6 and p.Asp59Gly, respectively.

We tested these *gbh-1* variants under various nutritional conditions to determine whether and what type of phenotype they produce and whether there is a specific association of the produced phenotype with L-carnitine deficiency and γ -BB accumulation.

As shown in our experiments with the *gbh-1*(*ko*) variant, the complete absence of GBH-1 causes reduced embryonic viability upon standard feeding and starving conditions, which is reversible upon enhanced feeding and L-carnitine supplementation upon refeeding conditions. The same phenotype was observed in the *gbh-1*(G283R) and *gbh-1*(G247Vfs*6) variant nematodes, indicating that *gbh-1*(G283R) and *gbh-1*(G247Vfs*6) are pathogenic functional alleles comparable to the knockout allele.

To mitigate the challenge in correlating genotype and phenotype in the L-carnitine metabolic pathway, which is influenced by both exogenous supply and endogenous synthesis, we refined our *C. elegans* model by carefully controlling the external source of L-carnitine by introducing the *E. coli* mutant, BW25113 (Δ *caiA*), which is not able to synthesize L-carnitine. Under this selective exogenous L-carnitine deficiency, we found profound embryonic lethality both in the *gbh-1*(*ko*) knockout allele as well as in the *gbh-1*(G283R) and *gbh-1*(G247Vfs*6) variants. The complete reversibility of these findings upon L-carnitine supplementation provided robust evidence for the intrinsic effects of BBOX1 on L-carnitine bioavailability. The same phenotype was observed upon selective accumulation of γ -BB by adding high concentrations of γ -BB to wild-type BW25113, which is able to synthesize L-carnitine. These findings indicate that the phenotypic observation of reduced embryonic vitality is specifically due to L-carnitine deficiency and accumulation of γ -BB. Translating results from the nematode model to human disease further allows the assumption that both L-carnitine deficiency and accumulation of γ -BB play an independent but synergistic role in the pathogenesis of human BBOX1 deficiency.

The growth characteristics of Δ *caiA*, mirroring those of the parental strain BW25113 in both liquid culture and on agar plates, indicate that the observed embryonic lethality stems not from restricted bacterial growth or nutritional scarcity but from the specific absence of L-carnitine synthesis capability in both the worm mutant and Δ *caiA*. Hence, it is evident that

L-carnitine production within *E. coli* plays a pivotal role in supplying essential exogenous L-carnitine, compensating for the impaired endogenous synthesis in *C. elegans* due to mutations in *gbh-1*. This crucial support is independent of the nutritional conditions. As a result, the BW25113 strain and its Δ *caiA* mutant have become vital to our maintenance of *gbh-1* mutants and subsequent assessments of γ -BB toxicity and metabolic studies, as the WT strain supports growth and embryonic viability, and the Δ *caiA* mutant strain supports growth (for one generation), yet does not support embryonic viability.

In contrast to the *gbh-1*(G283R) and *gbh-1*(G247Vfs*6) variants, the *gbh-1*(D72G) did not show an obvious phenotype upon the various nutritional conditions described above. Particularly, when expressed as a compound heterozygous with the clearly defined pathogenic variant *gbh-1*(G247Vfs*6), we observed no embryonic lethality even under starvation conditions. These results suggest that GBH-1(D72G) retains significant normal enzymatic function in worms, despite the high conservation of residue D72G. However, while the D72G variant does not result in reduced embryonic vitality, we were able to confirm its impact through metabolomic analysis, which showed a mild but consistent elevation in γ -BB levels. The mild elevation of γ -BB, coupled with a conserved amino acid change, suggests that D72G is a hypomorphic, milder variant resulting in a quantifiable metabolic phenotype where small deviations in γ -BB levels are metabolically tolerable in *C. elegans*.

Our experiments testing the sensitivity of *gbh-1* mutants to γ -BB toxicity offer insightful observations on the differential effects of BBOX1 variants. Specifically, the variants G247Vfs*6 and G283R exhibit embryonic lethality upon exposure to γ -BB at mM concentrations, closely mimicking the response observed in the knockout alleles. This pronounced vulnerability, even in the presence of the carnitine-producing *E. coli* strain that served as a nutritional source, points to primary γ -BB toxicity. Although *E. coli* is known to produce γ -BB and crotonobetaine along with L-carnitine¹⁹, the produced amounts are likely low and non-contributory to the observed toxic effects. Presumed mechanisms of toxicity could be chemical or by competitive inhibition of the carnitine transporter, which would further aggravate the intracellular carnitine deficiency. The observed insensitivity of the D72G variant to γ -BB exposure is in line with other phenotypic observations pointing to a milder variant. Residual L-carnitine production in a hypomorphic allele may provide intracellular L-carnitine levels high enough to protect against γ -BB-related toxicity, potentially caused by competitive inhibition of L-carnitine transport into the cells.

The metabolomic analysis of our *gbh-1* variants provided further insights into the biochemical consequences of deficient L-carnitine synthesis at the level of BBOX1. While we could demonstrate evidence of L-carnitine deficiency and accumulation of γ -BB as direct consequences of *gbh-1*/BBOX1 deficiency, the absence of significant changes in other metabolites confirms that the loss of GBH-1 selectively impacts the L-carnitine biosynthesis pathway without significantly affecting other metabolic pathways in amino acid, nucleotide, and energy metabolism that are not dependent on L-carnitine (Fig. S5F, Supplementary tables), underscoring the role of L-carnitine synthesis in the observed phenotypes.

Overall, through an integrated analysis of the phenotypic and metabolic characteristics in our nematode model, we clearly show a functional effect of all variants. Accumulation of γ -BB was observed in all variants G247Vfs*6, G283R, and D72G. Additional embryonic lethality and L-carnitine deficiency were observed in the G247Vfs*6 and G283R. The improvement of embryonic lethality upon L-carnitine supplementation and the demonstration of primary γ -BB toxicity in our *C. elegans* model provide important insights into treatment options for this condition.

Although findings in *C. elegans* provide a foundational understanding of the metabolic implications of BBOX1 variants, direct translation of this data to human conditions warrants caution. Human metabolism is influenced by a broader array of genetic, environmental, and dietary factors, which may modulate the clinical manifestations of similar genetic variants. Nevertheless, the observed sensitivity to γ -BB toxicity in these specific *gbh-1*

mutants highlights the potential for similar metabolic vulnerabilities in humans carrying equivalent *BBOX1* variants.

Methods

Patients

Ethical approval for this study was provided by the Children's and Women's Health Center of British Columbia Research Ethics Board (H21-03927, H18-02853, and H18-00726). Informed consent was obtained from all participants. We have complied with all relevant ethical regulations, including the Declaration of Helsinki. Whole-genome sequencing was performed in the Silent Genomes Project for Patient 3. Sanger sequencing for segregation of *BBOX1* variants in Patient 2 was performed in the Rare Disease Discovery Hub project (<https://www.bcchr.ca/thehub>).

Serum and dried blood spot acylcarnitine profile

Acylcarnitine profiles were tested in serum and dried blood spot samples at the Biochemical Genetics Laboratory at BC Children's Hospital according to the standard clinical protocols.

Carnitine biosynthesis intermediates measurement

Measurements of carnitine biosynthesis intermediates, including N-6-trimethyllysine, gamma-butyrobetaine, and HTML/TML ratio, were performed at the Amsterdam UMC laboratory for Genetic Metabolic Diseases in Amsterdam, the Netherlands.

Strains and culture conditions

C. elegans strains were obtained from Caenorhabditis Genetics Center (CGC) and/or generated in the lab (Table 2). Worms were conventionally maintained on *E. coli* OP50 seeded NGM plates (thin OP50 plates) at 20 °C as outlined²⁰. To make thin OP50 plates, 0.05 mL overnight OP50 culture was applied and spread onto NGM plates (60 mm). To make thick OP50 plates, 0.05 mL 5 times concentrated overnight OP50 culture was applied and spread onto NGM plates. Mutant strains and control wild-type N2 strains were maintained on thick OP50 plates or BW25113 at 20 °C before experiments. The *E. coli* OP50 strain was a gift from Dr. Paul Mains, while *E. coli* HB101 strain was a gift from Dr. James McGhee. *E. coli* BW25113 and BW25113(*ΔcaiA*), part of the *E. coli* Keio Knockout Collection²¹ were gifts from Drs. Alexei Savchenko and Nobuhiko Watanabe at the University of Calgary.

Liquid culture of *C. elegans* for metabolic extraction

For metabolic extraction from *C. elegans*, synchronized L1 larvae were obtained through settling starved L1 animals, followed by a dual settling process to enrich for L1 stage larvae as described previously²². Cultures were grown on NGM plates with *E. coli* BW25113 at 20 °C. For metabolomic sample preparation, approximately 30,000 L1 larvae were cultured in 5 mL K medium²² supplemented with adjusted salt concentrations, cholesterol, kanamycin, and BW25113(*ΔcaiA*) in a T25 tissue culture flask. The flasks were incubated at 23 °C with orbital shaking until larvae reached the young adult stage. Subsequently, animals and culture medium were separated via centrifugation, and the medium and worm pellet were frozen for LC-MS.

Metabolic extraction

Approximately 30,000 adult worms or 5 mL of culture medium per sample were processed. The samples were homogenized using a motorized pestle on dry ice, followed by the addition of ice-cold 90% methanol for worms or a 1:2 dilution with 100% methanol for the medium. After incubation on ice for 30 min and subsequent centrifugation at 4000 × g (worms) or maximum speed (~21,000 × g for medium) for 10–15 min at 4 °C, the supernatants were transferred to pre-chilled microcentrifuge tubes, concentrated via SpeedVac, and resuspended in 50% methanol. These extracts were stored at –80 °C until mass spectrometry analysis, ensuring no visible debris was present to avoid complications in UHPLC systems. Samples were delivered on dry ice for analysis, with a methanol/water mix used for dilution before MS processing.

Metabolic analysis of *C. elegans* metabolic extracts

This method has been adopted from previously published studies^{23–25}. Metabolic analysis was performed on a Q Exactive™ HF Hybrid Quadrupole-Orbitrap™ Mass Spectrometer (Thermo Fisher) coupled to a Vanquish™ UHPLC System (Thermo Fisher). Chromatographical separation of metabolites was performed on Syncronis HILIC UHPLC column (2.1 mm × 100 mm × 1.7 μm, Thermo Fisher) at the flow rate of 600 μL/min using a binary solvent system: solvent A, 20 mM ammonium formate, pH 3.0 in mass spectrometry grade H₂O, and solvent B, mass spectrometry grade acetonitrile with 0.1% formic acid (%v/v). The following gradient was used: 0–2 min, 100%B; 2–7 min, 100–80%B; 7–10 min, 80–5%B; 10–12 min, 5%B; 12–13 min, 5–100%B; 13–15 min, 100%B. Sample injection volume was 2 μL. The mass spectrometer was run in positive full scan mode at a resolution of 240,000, scanning from 50 to 750 m/z. Metabolite data is analyzed by the EL-MAVEN software package^{26,27}. Metabolites were identified by matching observed m/z signals (±10 ppm) and chromatographic retention times to those observed from commercial metabolite standards (LMSLS™ Sigma-Aldrich). Next, metabolites were quantified by comparison to an eight-point quantification curve of metabolite standards.

Data availability

Data collected and analyzed for this manuscript are available upon request.

Received: 28 March 2025; Accepted: 8 September 2025;

Published online: 29 September 2025

References

1. Longo, N., Frigeni, M. & Pasquali, M. Carnitine transport and fatty acid oxidation. *Biochim. Biophys. Acta* **1863**, 2422–2435 (2016).
2. Nezu, J. et al. Primary systemic carnitine deficiency is caused by mutations in a gene encoding sodium ion-dependent carnitine transporter. *Nat. Genet.* **21**, 91–94 (1999).
3. Vaz, F. M. & Wanders, R. J. A. Carnitine biosynthesis in mammals. *Biochem. J.* **361**, 417–429 (2002).
4. Rebouche, C. J. & Engel, A. G. Tissue distribution of carnitine biosynthetic enzymes in man. *Biochim. Biophys. Acta* **630**, 22–29 (1980).
5. Almannai, M., Alfadhel, M. & El-Hattab, A. W. Carnitine Inborn Errors of Metabolism. *Molecules* **24**, 3251 (2019).
6. Celestino-Soper, P. B. S. et al. Use of array CGH to detect exonic copy number variants throughout the genome in autism families detects a novel deletion in TMLHE. *Hum. Mol. Genet.* **20**, 4360–4370 (2011).
7. Celestino-Soper, P. B. S. et al. A common X-linked inborn error of carnitine biosynthesis may be a risk factor for nondysmorphic autism. *Proc. Natl. Acad. Sci. USA* **109**, 7974–7981 (2012).
8. Rashidi-Nezhad, A., Talebi, S., Saebnouri, H., Akrami, S. M. & Reymond, A. The effect of homozygous deletion of the *BBOX1* and *Fibin* genes on carnitine level and acyl carnitine profile. *BMC Med. Genet.* **15**, 75 (2014).
9. Sinclair, G. B. et al. Carnitine palmitoyltransferase I and sudden unexpected infant death in British Columbia First Nations. *Pediatrics* **130**, e1162–e1169 (2012).
10. Collins, S. A. et al. Carnitine palmitoyltransferase 1A (CPT1A) P479L prevalence in live newborns in Yukon, Northwest Territories, and Nunavut. *Mol. Genet. Metab.* **101**, 200–204 (2010).
11. Sim, N.-L. et al. SIFT web server: predicting effects of amino acid substitutions on proteins. *Nucleic Acids Res.* **40**, W452–W457 (2012).
12. Adzhubei, I., Jordan, D. M. & Sunyaev, S. R. Predicting functional effect of human missense mutations using PolyPhen-2. *Curr. Protoc. Hum. Genet.* **7**, 20 (2013).
13. Schubach, M., Maass, T., Nazaretyan, L., Röner, S. & Kircher, M. CADD v1.7: using protein language models, regulatory CNNs and other nucleotide-level scores to improve genome-wide variant predictions. *Nucleic Acids Res.* **52**, D1143–D1154 (2024).

14. Yilmaz, L. S. & Walhout, A. J. M. A *Caenorhabditis elegans* genome-scale metabolic network model. *Cell Syst.* **2**, 297–311 (2016).
15. Elssner, T., Preusser, A., Wagner, U. & Kleber, H. P. Metabolism of L(-)-carnitine by Enterobacteriaceae under aerobic conditions. *FEMS Microbiol. Lett.* **174**, 295–301 (1999).
16. Dall, K. B., Havelund, J. F., Harvald, E. B., Witting, M. & Faergeman, N. J. HLH-30-dependent rewiring of metabolism during starvation in *C. elegans*. *Aging Cell* **20**, e13342 (2021).
17. Lee, H. et al. BBOX1 is down-regulated in maternal immune-activated mice and implicated in genetic susceptibility to human schizophrenia. *Psychiatry Res.* **259**, 197–202 (2018).
18. Vaz, F. M., van Gool, S., Ofman, R., Ijlst, L. & Wanders, R. J. Carnitine biosynthesis: identification of the cDNA encoding human gamma-butyrobetaine hydroxylase. *Biochem. Biophys. Res. Commun.* **250**, 506–510 (1998).
19. Meadows, J. A. & Wargo, M. J. Carnitine in bacterial physiology and metabolism. *Microbiology* **161**, 1161–1174 (2015).
20. Brenner, S. The genetics of *Caenorhabditis elegans*. *Genetics* **77**, 71–94 (1974).
21. Baba, T. et al. Construction of *Escherichia coli* K-12 in-frame, single-gene knockout mutants: the Keio collection. *Mol. Syst. Biol.* **2**, 2006.0008 (2006).
22. Fox, B. W. et al. *C. elegans* as a model for inter-individual variation in metabolism. *Nature* **607**, 571–577 (2022).
23. Mager, L. F. et al. Microbiome-derived inosine modulates response to checkpoint inhibitor immunotherapy. *Science* **369**, 1481–1489 (2020).
24. Dong, X. et al. Thermogenic hydrocarbon biodegradation by diverse depth-stratified microbial populations at a Scotian Basin cold seep. *Nat. Commun.* **11**, 5825 (2020).
25. Rydzak, T. et al. Metabolic preference assay for rapid diagnosis of bloodstream infections. *Nat. Commun.* **13**, 2332 (2022).
26. Clasquin, M. F., Melamud, E. & Rabinowitz, J. D. LC-MS data processing with MAVEN: a metabolomic analysis and visualization engine. *Curr. Protoc. Bioinform.* **14**, 11 (2012).
27. Melamud, E., Vastag, L. & Rabinowitz, J. D. Metabolomic analysis and visualization engine for LC-MS data. *Anal. Chem.* **82**, 9818–9826 (2010).
28. Caspi, R. et al. The MetaCyc database of metabolic pathways and enzymes - a 2019 update. *Nucleic Acids Res.* **48**, D445–D453 (2020).

Acknowledgements

We gratefully acknowledge the patients and their families for participation in this study. We are thankful to our Silent Genomes Team for the Indigenous Background Variant Library, as well as the Silent Genomes Indigenous Rare Disease Diagnosis (S-GIRDD) Steering Committee for providing very helpful and thoughtful insights. We thank Catherine Diao for helping with *C. elegans* general handling and maintenance procedures. Metabolomics data were acquired by D.B. and M. D. at the Calgary Metabolomics Research Facility (CMRF), which is supported by the International Microbiome Centre and the

Canada Foundation for Innovation. Finally, we thank our funding sources: Genome Canada and Genome BC (275SIL and 298SGC), Canadian Institutes of Health Research (GP1-155868), BC Children's Hospital Research Institute and BC Children's Hospital Foundation, Illumina (in-kind), Provincial Health Services Authority, Alberta Children's Hospital Foundation and Canadian "Rare Diseases: Models & Mechanisms" Network (RDMM).

Author contributions

Conceived and designed the experiments: X.L., M.Y., G.H., M.T.G., and S.S.I. Performed the experiments: X.L., J.M., B.R., and F.M.V. Analyzed the data: X.L., M.Y., G.S., J.M., L.A., A.L., B.R., F.M.V., G.H., M.T.G., and S.S.I. Contributed to the clinical assessment of the probands: M.Y., K.J., L.A., A.L., G.H., and S.S.I. Wrote the paper: X.L., M.Y., M.T.G., and S.S.I. A critical review of the manuscript: G.S., J.M., K.J., L.A., A.L., B.R., F.M.V., and G.H.

Competing interests

The authors declare no competing interests.

Additional information

Supplementary information The online version contains supplementary material available at <https://doi.org/10.1038/s41525-025-00523-2>.

Correspondence and requests for materials should be addressed to Maja Tarailo-Graovac or Sylvia Stockler-Ipsiroglu.

Reprints and permissions information is available at <http://www.nature.com/reprints>

Publisher's note Springer Nature remains neutral with regard to jurisdictional claims in published maps and institutional affiliations.

Open Access This article is licensed under a Creative Commons Attribution-NonCommercial-NoDerivatives 4.0 International License, which permits any non-commercial use, sharing, distribution and reproduction in any medium or format, as long as you give appropriate credit to the original author(s) and the source, provide a link to the Creative Commons licence, and indicate if you modified the licensed material. You do not have permission under this licence to share adapted material derived from this article or parts of it. The images or other third party material in this article are included in the article's Creative Commons licence, unless indicated otherwise in a credit line to the material. If material is not included in the article's Creative Commons licence and your intended use is not permitted by statutory regulation or exceeds the permitted use, you will need to obtain permission directly from the copyright holder. To view a copy of this licence, visit <http://creativecommons.org/licenses/by-nc-nd/4.0/>.

© The Author(s) 2025